



Published in final edited form as:

Nature. 2013 March 7; 495(7439): 116–120. doi:10.1038/nature11942.

## Non-optimal codon usage is a mechanism to achieve circadian clock conditionality

Yao Xu<sup>1</sup>, Peijun Ma<sup>1</sup>, Premal Shah<sup>2</sup>, Antonis Rokas<sup>1</sup>, Yi Liu<sup>3</sup>, and Carl Hirschie Johnson<sup>1,\*</sup>

<sup>1</sup>Department of Biological Sciences, Vanderbilt University, Nashville, TN 37235 USA

<sup>2</sup>Department of Biology, University of Pennsylvania, Philadelphia, PA 19104 USA

<sup>3</sup>Department of Physiology, The University of Texas Southwestern Medical Center, Dallas, TX 75390 USA

### Abstract

Circadian rhythms are oscillations in biological processes that function as a key adaptation to the daily rhythms of most environments. In the model cyanobacterial circadian clock system, the core oscillator proteins are encoded by the gene cluster *kaiABC*<sup>1</sup>. Genes with high expression and functional importance like the *kai* genes are usually encoded by optimal codons, yet the codon usage bias of the *kaiBC* genes is not optimized for translational efficiency. We discovered a relationship between codon usage and a general property of circadian rhythms called conditionality; namely, that endogenous rhythmicity is robustly expressed under some environmental conditions but not under others<sup>2</sup>. Despite the generality of circadian conditionality, however, its molecular basis is unknown for any system. Here we show that non-optimal codon usage was selected as a post-transcriptional mechanism to switch between circadian and non-circadian regulation of gene expression as an adaptive response to environmental conditions. When the *kaiBC* sequence was experimentally optimized to enhance expression of the KaiB and KaiC proteins, intrinsic rhythmicity was enhanced at cool temperatures that are experienced by this organism in its natural habitat. However, fitness at those temperatures was highest in cells whose endogenous rhythms were suppressed at cool temperatures as compared with cells exhibiting high-amplitude rhythmicity. These results indicate natural selection against circadian systems in cyanobacteria that are intrinsically robust at cool temperatures. Modulation of circadian amplitude is therefore critical to its adaptive significance<sup>3</sup>. Moreover, these results show the direct effects of codon usage on a complex phenotype and organismal fitness. Our work also challenges

Users may view, print, copy, download and text and data- mine the content in such documents, for the purposes of academic research, subject always to the full Conditions of use: [http://www.nature.com/authors/editorial\\_policies/license.html#terms](http://www.nature.com/authors/editorial_policies/license.html#terms)

\*corresponding author: Dr. Carl Johnson, Dept. of Biological Sciences, Vanderbilt University, 465 21st Ave. South, Nashville, TN 37235 USA, TEL: 615-322-2384, FAX: 615-936-0205, [carl.h.johnson@vanderbilt.edu](mailto:carl.h.johnson@vanderbilt.edu).

**Full Methods** and any associated references are available in the online version of the paper at [www.nature.com/nature](http://www.nature.com/nature).

**Author Contributions** Y.X. and P.M. collected data; Y.X., P.M., and Y.L. analysed the experimental data; Y.X., P.S. and A.R. analysed the bioinformatic data; Y.L. and C.H.J. designed the original conceptual basis for the study, Y.X. and C.H.J. designed the experimental bases for the study; Y.X., P.S., and C.H.J. wrote the manuscript. All authors discussed the results and commented upon the manuscript.

Reprints and permissions information is available at [www.nature.com/reprints](http://www.nature.com/reprints).

The authors declare no competing financial interests.

Supplementary Information is linked to the online version of the paper at [www.nature.com/nature](http://www.nature.com/nature).

the long-standing view of directional selection towards optimal codons<sup>4–7</sup>, and provides a key example of natural selection against optimal codon to achieve adaptive responses to environmental changes.

---

Most amino acids are encoded by multiple codons, and species vary in their preferences for specific codons for the same amino acid. This preference, or codon usage bias, is thought to reflect a balance between mutational biases and selection for translational efficiency and accuracy<sup>4,6–9</sup>. Although the relative importance of various factors affecting codon usage is debated<sup>10,11</sup>, the degree of codon usage bias is known to increase with higher gene expression<sup>12</sup>. In particular, genes under stronger selection for translational efficiency and/or accuracy show greater preference for using codons whose complementary tRNAs have higher abundances. Despite the fact that codon usage bias is a strong indicator of selection on genes<sup>13</sup> and that the specific nature of codon bias can be changed by environmental factors such as temperature and hyper-salinity<sup>14,15</sup>, its direct effect on a complex phenotype and organismal fitness remains largely unknown.

In the cyanobacterium *Synechococcus elongatus* PCC7942, circadian rhythms confer a strong selective advantage in rhythmic environments<sup>3,16</sup>. In *S. elongatus*, expression of the entire genome is controlled by the circadian pacemaker, as shown by rhythms of promoter activity<sup>17</sup>, mRNA abundance<sup>18–20</sup>, and the topology of the entire chromosome<sup>19,21</sup>. The core circadian clock is composed of three components, KaiA, KaiB, and KaiC, that are expressed as monocistronic *kaiA* and dicistronic *kaiBC* transcripts<sup>1</sup>. Both transcripts are expressed at very high levels, falling within the top 5% of mRNA abundances in *S. elongatus*<sup>18,19</sup>. Whereas initial examination of codon usage in *kaiBC* suggested an unusual codon bias (Table S1, Fig. 1a), further analyses indicated that amino acid specific codon usage in *kaiB* and *kaiC* is not significantly different from that of the average codon usage in the rest of the genome (Fig. 1b). In order to quantify the degree of selection on the *kai* gene cluster, we focused upon its codon adaptation index (CAI)<sup>13</sup> and the 5' mRNA folding energies of its transcripts. Given that *kaiBC* transcripts are very highly abundant, it was surprising that the CAI for *kaiB* and *kaiC* is less than the average CAI value of all *S. elongatus* genes (Fig. 1b). Moreover, even though the folding energy of the *kaiB* transcript is less negative than that for most transcripts (Fig. 1c)—indicating that it has a relatively weaker secondary structure than most mRNAs in this organism and is therefore likely to initiate translation efficiently—the weak secondary structure of the *kaiB* transcript is insufficient to account for its high mRNA abundance given that the CAI is considerably below average. The *kaiC* portion of the *kaiBC* transcript has similar CAI (Fig. 1b) and folding energy (Fig. 1c) values as those of the *kaiB* portion.

To test whether the lower CAI of *kaiBC* might be adaptive in the core clock mechanism and/or in the output pathways controlled by the pacemaker in cyanobacteria, we generated two strains whose endogenous *kaiBC* gene was replaced with modified versions of *kaiBC* in which codon usage was “optimized” to be similar to that of highly expressed genes<sup>18,19</sup>, thereby increasing their CAI values from 0.60 to 0.95 for *kaiB* and 0.61 to 0.82 for *kaiC* (Fig. 1a; Tables S2 and S3). Changing the codon usage of a gene in its 5' region affects its folding energy and hence its rate of translation initiation<sup>8,22–24</sup>. Indeed, the optimized

versions of *kaiB* and *kaiBC* also had significantly lower 5' folding energy of the *kaiBC* transcript (Figs. 1c & 1d). Because the *kaiBC* gene is transcribed as a single discistronic mRNA with *kaiB* at its 5' end<sup>1</sup>, one optimized strain ("optKaiB") replaced the entire *kaiB*<sup>WT</sup> gene with an optimized *kaiB*<sup>opt</sup>, whereas the other optimized strain ("optKaiBC") replaced both the *kaiB*<sup>WT</sup> gene and the 5' half of the *kaiC*<sup>WT</sup> gene with optimized versions (*kaiB*<sup>opt</sup> and *kaiC*<sup>opt</sup>, Fig. 2a). Our initial hypothesis was that the "non-optimal" codon bias of the endogenous *kaiBC* is essential for the expression of circadian rhythmicity, which would predict that the intrinsic rhythmicity of optKaiB and optKaiBC strains would be poorer than that of wild-type (as is true for the studies of *Neurospora* FRQ, accompanying manuscript by Zhou *et al.*). Unexpectedly, the observed circadian rhythms of gene expression in the optKaiB and optKaiBC strains were as robust as those of the wild-type *S. elongatus* at the optimal growth temperature of 30°C (Fig. 2b). However, to be adaptive, circadian clocks must be able to keep time accurately over the range of physiological temperatures for a given organism<sup>25</sup>, so we tested real-time gene expression profiles of the optimized strains relative to WT at temperatures from 18°C to 38°C. Again, to our surprise the optKaiB and optKaiBC strains exhibited robustly rhythmic gene expression over a broad range of temperatures (Fig. 2b, Table S4). In contrast, the rhythm of WT damps within a few cycles at cool temperatures (18–23°C, Fig. 2b, Table S4). There are no significant differences in the free-running period of the circadian rhythms between WT and optKaiB/optKaiBC at 18–20°C and 26–32°C, and only small differences at other temperatures within the 18–38°C range (Fig. 2c). Overall, the temperature compensation of the optimized strains was slightly poorer ( $Q_{10} \sim 1.13$ ) over the range of 23–36°C than that for WT ( $Q_{10} \sim 1.10$  from ref. 26, and  $Q_{10} \sim 1.04$  from Fig. 2c and Table S6), which might relate to the difference in mRNA folding energies (Fig. 1d).

We further confirmed that improved rhythmicity at lower temperatures of the optKaiB and optKaiBC strains (Fig. 2b) was due to higher protein production levels of KaiB and KaiC. First, Figs. 3a and Supplementary Fig. S1 confirm that KaiC levels are considerably higher in the optKaiBC strain as compared with WT, and Figs. 3b and Supplementary Fig. S2 show that KaiB levels are similarly elevated in both the optKaiB and optKaiBC strains. Interestingly, the amplitude of the KaiC phosphorylation rhythm is comparable between WT and optKaiBC at 20°C (Fig. 3a). Second, to validate that the augmented KaiB and/or KaiC levels were responsible for the improved rhythmicity at cool temperatures, we co-expressed the native (non-optimized) sequences of *kaiB* (strain KaiB<sup>WT/OX</sup>) or *kaiBC* (strain KaiBC<sup>WT/OX</sup>) from an IPTG-inducible *trc* promoter to enhance endogenous production of KaiB and KaiC (Fig. 3c). Fig. 3d shows that KaiB is overexpressed in the KaiB<sup>WT/OX</sup> and the KaiBC<sup>WT/OX</sup> strains even in the absence of the IPTG inducer (due to the *trc* promoter being slightly leaky<sup>27</sup>), while KaiC levels are not altered. In the presence of a very low concentration of the inducer (5 μM IPTG), KaiB levels are enhanced in KaiB<sup>WT/OX</sup> and both KaiB and KaiC levels are increased in KaiBC<sup>WT/OX</sup> (Fig. 3d). KaiA levels are not substantially affected under any of these conditions. In rhythm assays at 18°C, optKaiB and optKaiBC exhibit improved rhythmicity as compared with WT as noted above, but so does the KaiBC<sup>WT/OX</sup> strain in the absence and presence of the inducer IPTG (Fig. 3e, Table S5). (Much higher concentrations of IPTG lead to arrhythmicity as noted before<sup>1,27</sup>; see Supplemental Figure S3.) Moreover, while the data depicted in Figure 3e are normalized

luminescence data, un-normalized data for an equivalent experiment at 20°C are shown in Supplemental Figure S4. On the other hand, the rhythm of the KaiB<sup>WT/OX</sup> strain damps rapidly. There is a clear correlation between the strains that exhibit sustained rhythmicity in constant conditions (an indicator of the endogenous circadian system) and a favorable KaiB abundance relative to KaiC abundance (optKaiB, optKaiBC, KaiBC<sup>WT/OX</sup>) versus the strains whose rhythmicity damps rapidly and express either a low KaiB level (WT) or a high KaiB level (KaiB<sup>WT/OX</sup>) relative to KaiC level (Fig. 3d,e). These experimental manipulations of KaiB and KaiC levels using non-optimized sequences strongly suggest that codon optimization of *kaiB* and *kaiC* affects the robustness of rhythmicity at cool temperatures primarily by affecting KaiB and KaiC expression, thereby altering the relative levels of KaiB, KaiC, and KaiA protein abundances in the cells. The stoichiometry among the Kai proteins is known to be critical for expression of the cyanobacterial *in vitro* oscillator<sup>28</sup>, and it is therefore likely to be a key determining factor in the expression of rhythmicity *in vivo* that we report here.

If alternative (*i.e.*, “optimal”) *kaiBC* sequences promote rhythmicity at cooler temperatures, why have they not been naturally selected? While 30°C is the optimal growth temperature for *S. elongatus* (Supplemental Fig. 5), 18–23°C is certainly a temperature range that this freshwater, temperate cyanobacterium could experience in its environment. We therefore tested the growth rates of *S. elongatus* in light/dark cycles at 37°C, 34°C, 30°C, 25°C, 20°C, and 18°C (Fig. 4 and Supplemental Figure S5). Consistent with our previous results using competition assays between WT and the arrhythmic strain CLAb as well as with the highly damped strain CLAc<sup>3</sup> (both CLAb and CLAc result from point mutations in the *kaiC* gene<sup>1</sup>), WT grew at a faster rate in LD at 30°C than CLAb or CLAc (Fig. 4b, Supplemental Table S7). The optKaiBC strain grew at about the same rate as WT or perhaps slightly faster. At cooler temperatures, however, the results were dramatically different. At 18°C and 20°C when the circadian rhythm of gene expression is damped in WT (Figs. 2b, 3e, Supplemental Fig. S4), WT grew significantly faster than optKaiBC (Fig. 4d,e, Supplemental Table S7). Even the arrhythmic CLAb and damped CLAc strains outperformed optKaiBC at 18–25°C (Fig. 4c-e, Supplemental Table S7). Therefore, at cool temperatures in LD cycles, strains having damped (WT, CLAc) or arrhythmic (CLAb) phenotypes under free-running conditions outgrew the strain that expressed robust rhythms (optKaiBC).

Biases in codon usage are generally thought to be under directional selection for an optimal balance between translational efficiency and accuracy, whereby a higher CAI is always better<sup>5,7</sup>. Other examples of selection for non-optimal codon usage (mediated by mRNA secondary structure and/or tRNA availability) are rare and poorly characterized<sup>8,29</sup>. Our study presents a counter-example to the standard view and suggests the action of either (i) selection against optimal codon usage or (ii) stabilizing selection where both low and high extremes in codon usage bias have higher fitness costs. Indeed, the non-optimal codon usage appears to be a molecular mechanism whereby post-transcriptional events allow *S. elongatus* cells to switch between circadian and non-circadian regulation of gene expression depending upon the environmental conditions, and our results harken back to earlier observations of such “conditionality” for circadian rhythms<sup>2,30</sup>.

Why is conditionality an important characteristic of circadian rhythms? We tend to think of circadian clocks as rhythmic *activators*, but they are also rhythmic *repressors*. Under some conditions this repressor/activator balance may inhibit growth and circadian regulation may not be adaptive. At cooler temperatures, the free-running period of the circadian rhythm of *S. elongatus* can be as long as 30 h (Fig. 2c), suggesting that the coupling of gene expression and rhythmic regulation might be maladaptive for growth at lower temperatures. For example, we previously reported that *S. elongatus* mutant strains with 30 h periods can entrain to 24 h light/dark cycles, but they do so with a significantly later phase relationship that is maladaptive<sup>16</sup>; that result dovetails with our current observations. As another example of conditionality, our previous competition experiments at 30°C found that the arrhythmic CLAb strain is more fit than WT under constant illumination, but it is rapidly outcompeted by WT in LD cycles<sup>3</sup> (and Fig. 4 also shows that the growth of CLAb is poorer than WT in LD cycles at 20–30°C). Therefore, both illumination and temperature are environmental parameters that demonstrate the “conditional” advantages of circadian regulation under some conditions but not under others.

Our data show that optimizing the codon usage for the circadian *kaiBC* genes of *S. elongatus* does not disrupt endogenous circadian regulation (as in the case of *Neurospora* FRQ, accompanying manuscript by Zhou *et al.*), but instead the sequence optimization enhances circadian regulation in a range of cool temperatures that are relevant for the ecology of this organism. Despite this enhancement of intrinsic rhythmicity, however, optimal codon usage at the *kai* locus impairs cell growth at cooler temperatures. Therefore, our data suggest selection against an optimal codon usage because it is incompatible with a post-transcriptionally modulated conditional suppression of circadian rhythmicity at cool temperatures. In *S. elongatus*, circadian “conditionality” allows expression of robust endogenous rhythmicity within the range of temperature that permits vigorous growth and suppresses rhythmicity at temperatures where growth of this species is minimal (Supplemental Fig. 5). Our observations provide a novel example of post-transcriptional regulation of circadian clock genes that confers an adaptive response to different environmental conditions.

## METHODS

### Evaluation of codon usage

To evaluate frequency of codon usage of the central clock genes *kaiABC*, we analyzed coding sequences from different groups. One group is from 2400255 residue sequences from all putative proteins within the whole genome of *Synechococcus elongatus* PCC 7942. The second group is from all 59 ribosomal genes in the genome (Table S2). We also analyzed microarray datasets from two independent labs<sup>18,19</sup>. First, we calculated total microarray signals from one circadian cycle in constant light (LL) for each of these genes. Then, all of these genes were rearranged from strongest to weakest mRNA abundances based on the total microarray signal values in LL. Finally, we selected the top 16 genes that show high microarray values from *both* datasets (Table S3), and combined all of these coding sequences to the third group as putative highly expressed genes. The codon usage frequency was analyzed with a web-based program from The Sequence Manipulation Suite of

Bioinformatics Organization, Inc. (Hudson, Massachusetts) (<http://www.bioinformatics.org>). The fractions of codon usage were based on usage frequencies per 1000 codons (Table S1).

### Codon optimization of *kai* genes

Relative synonymous codon usage (RSCU) is defined as the ratio of the observed frequency of codons to the expected frequency given that all the synonymous codons for the same amino acids are used equally<sup>13,31</sup>. In the absence of any codon usage bias, the RSCU value would be 1.00. A codon that is used less frequently than expected will have a value of less than 1.00 and *vice versa* for a codon that is used more frequently than expected. The overall RSCU values of *Synechococcus elongatus* PCC 7942 were calculated from 3261 coding sequences (990021 codons) from the genome (Table S8). Infrequently used codons in *kaiB* or *kaiC* coding sequences were changed to those coding for the specific amino acids with higher RSCU values (Table S9 and Table S10) or higher codon-usage fractions (Table S1) in the genome. As shown in Fig. S6 and Table S9, 67 out of 102 codons were optimized for the entire *kaiB* coding region, whereas for *kaiC* gene, the infrequently-used codons were mainly optimized in the N-terminal KaiC-I domain that is encoded by the 5' half of the *kaiC* gene (Fig. S7 and Table S10).

### Synthesis and construction of optimized *kai* genes

DNA fragments containing optimized *kaiB* or *kaiC* coding sequences with wild-type flanking sequences were commercially synthesized and cloned into the *Sma* I site of pUC57 (EZBiolab Inc., Westfield, IN) to produce pUCoptKaiB and pUCoptKaiC, respectively. Based on pUCoptKaiB and pUCoptKaiC templates, the *optKaiB* or *optKaiC* fragments were resynthesized using 12 ~18 thermal cycles with pfuUltra® High-fidelity DNA polymerase (Stratagene, San Diego, CA) and primers containing the corresponding wild-type flanking sequences. After purification, the *optKaiB* or *optKaiC* fragments were EZcloned (Stratagene, San Diego, CA) into a plasmid containing the wild type *kai* cluster DNA to replace the corresponding wild-type DNA sequences. After the unchanged parental plasmid was digested at 37°C for 1 h with *Dpn* I (New England Biolabs, Beverly, MA), the circular, nicked optimized dsDNA was transformed into *E. coli* to generate pKai-optKaiB and pKai-optKaiC, respectively. To optimize both *kaiB* and *kaiC* genes, the resynthesized *optKaiB* fragment was EZcloned into the plasmid pKai-optKaiC to replace the corresponding wild-type *kaiB* coding sequences and to produce pKai-optKaiBC. All of these *kai*-optimized constructs were confirmed by DNA sequencing analysis. In case of direct comparison, the wild-type version of *kaiB*, *kaiC*, and *kaiBC* genes or coding sequences are indicated as *kaiB*<sup>WT</sup>, *kaiC*<sup>WT</sup>, and *kaiBC*<sup>WT</sup>, whereas the codon-optimized versions are denoted as *kaiB*<sup>opt</sup>, *kaiC*<sup>opt</sup>, and *kaiBC*<sup>opt</sup>, respectively.

### Computation of codon adaptation index (CAI) and 5' mRNA folding energy

In order to calculate CAI values of genes, we began by calculating the relative synonymous codon usage (RSCU) of all ribosomal genes (Table S2)<sup>13</sup>. Using these RSCU values, we calculated the CAI values of all genes in the *S. elongatus* genome and the codon-optimized versions of the *kai* genes. Using a sliding window of 20 codons, Figure 1a shows that optimized versions of both *kaiB* (*kaiB*<sup>opt</sup>) and *kaiC* (*kaiC*<sup>opt</sup>) genes have higher CAI values

along the entire length of the genes than the WT versions and higher than the average CAI of ribosomal genes. The CAI of the wild-type *kaiB* and *kaiC* genes is less than the average CAI of the genome, in spite of their high abundance in the transcriptome. As expected, the average CAI of ribosomal genes is much higher than the average. As an example, the CAI of *kaiB<sup>opt</sup>* was optimized to 0.95 as shown by the red line in Fig. 1b using the relative synonymous codon usage (RSCU) of ribosomal genes.

In addition to codon usage as it relates to the relative expression of various tRNA genes, the translational efficiency of a protein's production depends on the 5' folding energy of its mRNA (1–40 nc). To calculate the minimum free energy ( $\Delta G$ ) of folding of the 5' region of mRNAs, we used the first 40 nucleotides of the coding sequences (1–40 nc). In addition, we used the RNA folding algorithm in RNA fold of the Vienna RNA Package 2.0<sup>32</sup>. We calculated  $\Delta G$  at 37°C for each gene in the *S. elongatus* genome using default parameters. Then, to calculate the effect of temperature on folding energy for the *kai* genes (wild-type and optimized versions), we varied the temperature from 18°C – 40°C. The folding energy of the *kaiB<sup>WT</sup>* and *kaiC<sup>WT</sup>* genes is much higher than the rest of the genome, indicating selection for faster translation initiation (Fig. 1c). Since the folding energy of an mRNA depends on the temperature, calculation of the minimum free energy of folding ( $\Delta G$ ) at varying temperatures showed that the  $\Delta G$  for both *kaiB<sup>WT</sup>* and *kaiB<sup>opt</sup>* increases with temperature, and that optimizing codon usage also increases the  $\Delta G$  of the *kaiB<sup>opt</sup>* gene at all temperatures (Fig. 1d).

### Generation of *kai*-optimized and *kai*-coexpressing cyanobacterial strains

*Synechococcus elongatus* PCC 7942 was used as the cyanobacterial host strain. A *kaiBCp::luxAB* luminescence reporter of clock-controlled gene expression was integrated into either neutral site I (NS I) with a spectinomycin selection marker (or in other experiments, into NS II with a chloramphenicol selection marker), in which the expression of the *Vibrio harveyi* luciferase structure gene cassette *luxAB* is driven by the promoter of the *kaiBC* genes (*kaiBCp*) and serves as a real-time reporter of promoter activity<sup>1,26,27</sup>. The *kaiABC*-null strain was created by replacement of the *kaiABC* DNA region with a kanamycin resistance gene<sup>1</sup>. The wild-type *kaiABC* cluster or codon-optimized *kaiABC* cluster containing a *kaiB<sup>opt</sup>*, *kaiC<sup>opt</sup>*, or *kaiBC<sup>opt</sup>* coding region and a spectinomycin resistance cassette was reintroduced into the endogenous *kai* locus by replacing the kanamycin resistance gene of the *kaiABC*-null strain to give rise to transgenic strains with either the wild-type version of the *kaiABC* cluster or the optimized version of the *kaiABC* cluster. This replacement was done in such a way that the *kaiABC* cluster was recreated to be exactly as the wild-type cluster with no insertions or deletions except a selection marker downstream of the genomic *kaiC* sequence. The transgenic cyanobacterial strain harboring the wild-type version of the *kai* cluster was named the wild type strain (WT), whereas the strains harboring codon-optimized versions of the *kai* cluster with *kaiB<sup>opt</sup>*, *kaiC<sup>opt</sup>*, or *kaiBC<sup>opt</sup>* were called “optKaiB,” “optKaiC,” or “optKaiBC,” respectively (Fig. 2a). For co-expression of wild-type *kaiB*, *kaiC*, or *kaiBC* genes *in vivo*, the *trcp::kaiB<sup>WT</sup>*, *trcp::kaiC<sup>WT</sup>*, or *trcp::kaiBC<sup>WT</sup>* constructs with a kanamycin resistance marker<sup>27</sup> were transformed into the NS II region of a wild-type luminescence reporter strain to generate *kai*-coexpressing strains KaiB<sup>WT</sup>/OX, KaiC<sup>WT</sup>/OX, or KaiBC<sup>WT</sup>/OX (Fig. 3c), in which the coexpression of wild-

type *kaiB*, *kaiC*, or *kaiBC* genes from NSII were under the control of an IPTG-derepressible heterologous *trc* promoter and the original *kaiABC* cluster remains at the original wild-type site. These codon-optimized strains harboring *kaiB<sup>opt</sup>*, *kaiC<sup>opt</sup>*, or *kaiBC<sup>opt</sup>* and *kai*-coexpressing strains were confirmed by PCR, DNA sequencing, immunoblotting, as well as by luminescence analyses. As indicated in the diagrams of Fig. 2a, the wild-type coding region of *kaiB* gene was replaced with *kaiB<sup>opt</sup>* coding sequences in the optKaiB strain, whereas the *kaiBC* coding region was replaced with both *kaiB<sup>opt</sup>* and *kaiC<sup>opt</sup>* (i.e. *kaiBC<sup>opt</sup>*) coding sequences in the optKaiBC strain. At neutral site II (NS II), a *kaiBC* promoter-driving *luxAB* expression cassette with a chloramphenicol selection marker was integrated to function as a luminescence reporter of clock-controlled promoter activity. In the diagrams of Fig. 3c for the *kaiB<sup>WT</sup>*- or *kaiBC<sup>WT</sup>*-coexpressing strains, three sites in the chromosome are depicted: (i) the wild-type *kaiABC* cluster (*kaiABC<sup>WT</sup>*); (ii) the *luxAB* luminescence reporters in NS I; and (iii) an IPTG-derepressible promoter driving expression of *kaiB<sup>WT</sup>* (KaiB<sup>WT</sup>/OX strain) or *kaiBC<sup>WT</sup>* (KaiBC<sup>WT</sup>/OX strain) in NS II.

### Measurement of luminescence rhythms

Cyanobacterial strains were grown in modified BG11<sup>33</sup> liquid media with air bubbling or BG11 agar plates supplemented with appropriate antibiotics (spectinomycin, 20 µg/ml; kanamycin, 10 µg/ml; 5 µg/ml; chloramphenicol, 7.5 µg/ml) at 30°C under continuous cool-white illumination (LL; 40 ~ 50 µE/m<sup>2</sup> s). Before the cells were released into LL for the luminescence assay, a 12 h dark exposure was given to synchronize the rhythms of the individual cells in the population. For induction of coexpressed *kaiB*, *kaiC*, or *kaiBC* genes, the *trcp* inducer IPTG was added at LL0 to final concentrations of 0, 2, 5, 10, 100, or 1000 µM. Luminescence was measured with the *kaiBCp::luxAB* reporter of clock-controlled gene expression that serves as a real-time reporter of promoter activity<sup>1,26,27</sup>. For measurement of *in vivo* luminescence rhythms at different temperatures (18°C to 38°C), at least 12 independent colonies for each condition were monitored as previously described<sup>27,34</sup>. Our standard light intensity for the luminescence rhythm assay was 40 to 50 µE/m<sup>2</sup>s, but we observed that the rate of damping in WT was influenced by both the temperature (as described in this paper) and light intensity (as tested under a range of light intensities).

### Calculation of free-running period, Q10 value, and damping rate of luminescence rhythms

The period of luminescence rhythms was analyzed with ChronoAnalysis II, version 10.1 (courtesy of Dr. Till Roenneberg), and the Q<sub>10</sub> value for evaluation of temperature compensation over a wide range of temperatures was calculated with the following equation:  $Q_{10} = [(1/\tau_2)/(1/\tau_1)]^{10/(T_2-T_1)}$ ; where:  $\tau_1$  = period at the lower temperature (T<sub>1</sub>) and  $\tau_2$  = period at the higher temperature (T<sub>2</sub>)<sup>35</sup>. Damping rate is the number of days required for the amplitude of the rhythm to decrease to 1/e of the starting value. The damping rates were calculated with the LUMICYCLE data analysis program (Actimetrics, Evanston, IL; courtesy of D. Ferster). The program fits the data to a sine wave multiplied by an exponential decay factor<sup>36</sup>.



### Immunoblot assays for Kai abundance

After two LD 12:12 cycles, liquid cultures at  $OD_{750} \sim 0.3$  were released to constant light (LL) at indicated temperatures. About 30 ml of cells were harvested at different time points and an appropriate amount of fresh medium was added to the culture flask to maintain an equal cell density during the time course experiment. For *kaiB*- or *kaiBC*-coexpressing strains, the cultures were treated with or without 5  $\mu$ M of IPTG at LL0 for 12 hours before cell collection. Total proteins were extracted as previously described<sup>34</sup>. Total extracts were separated by SDS-polyacrylamide gel electrophoresis (PAGE) (15% gel for KaiB and 10% gel for KaiA and KaiC) and transferred onto nitrocellulose membranes. Proteins were transferred to nitrocellulose for immunoblotting using polyclonal rabbit antisera raised against KaiA or KaiB<sup>34</sup> or using polyclonal mouse antisera raised against KaiC<sup>27</sup>. Equal loading of extracts was confirmed by Coomassie Brilliant Blue (CBB) staining in the gel, Ponceau Red staining on the membrane, and/or by the density of nonspecific bands on the immunoblots. The immunoblot signals for relative Kai protein density/abundance were analyzed with NIH Image J software.

### Determination of growth rate and doubling time

Growth rates of cyanobacterial strains, including wild type, optKaiBC, as well as two arrhythmic/damped *kaiC* mutants (CLAb and CLAc)<sup>1,3</sup>, were measured in parallel at 18°C, 20°C, 25°C, 30°C, 34°C, and 37°C. Initial cultures were grown in liquid BG-11 medium at 30°C under constant illumination (50  $\mu$ E/m<sup>2</sup> s) in a shaking water bath at 100 rpm and with air bubbling into the cultures. Cell densities were monitored by measuring the optical density at 750 nm ( $OD_{750}$ ). When cell densities reached  $OD_{750} \sim 0.8$ , cultures were diluted to  $OD_{750} \sim 0.005$ , and grown in LD 12:12 cycles (12 hours light {50  $\mu$ E/m<sup>2</sup> s} followed by 12 hours darkness) in water baths set to 18°C, 20°C, 25°C, 30°C, 34°C, or 37°C with shaking (100rpm) and air bubbling. Cell densities were determined at  $OD_{750}$  over a time course as indicated. When  $OD_{750}$  values of cell cultures exceed 0.9, the OD measurement is not linear with cell density. Therefore, for samples with an  $OD_{750}$  that was larger than 0.9, the samples were diluted to an  $OD_{750}$  that was within the linear range before OD determination (and the plotted OD value then is corrected for the dilution). Two to six independent experiments were performed for each strain, and the growth curves were plotted as average  $OD_{750}$  values over time in LD. Doubling time was calculated by fitting exponential curves to the growth curves. Growth rate was generated by fitting growth data to exponential curves {cell density at a specific time = initial cell density  $\times e^{(\text{growth rate} \times \text{time})}$ }. (see: <http://mathworld.wolfram.com/LeastSquaresFittingExponential.html>). Doubling time was calculated as: Doubling time (hrs) =  $\{\ln(2)/\text{growth rate}\} \times 24$ .

### Statistical analyses

A two tailed Student t-test was used for statistical analyses. \*  $p < 0.05$ ; \*\*  $p < 0.01$ .

### Supplementary Material

Refer to Web version on PubMed Central for supplementary material.

## Acknowledgments

We are grateful for the suggestions of M. Woelfle and for the technical assistance of D. Zelli and C. Chintanaphol. This research was supported by grants from the National Institute of General Medical Science (N.I.H.) to CHJ (R01 GM067152 & R01 GM088595) and to YL (GM068496 & GM062591), the Welch Foundation (I-1560) to YL, the National Science Foundation to AR (DEB-0844968) and the Searle Scholars Program to AR. PS acknowledges support from a Burroughs Wellcome Fund Career Award and a David & Lucille Packard Foundation Fellowship awarded to Joshua B. Plotkin.

## References

1. Ishiura M, et al. Expression of a gene cluster *kaiABC* as a circadian feedback process in cyanobacteria. *Science*. 1998; 281:1519–1523. [PubMed: 9727980]
2. Njus D, McMurry L, Hastings JW. Conditionality of circadian rhythmicity: synergistic action of light and temperature. *J Comp Physiol*. 1977; 117:335–344.
3. Woelfle MA, Ouyang Y, Phanvijhitsiri K, Johnson CH. The adaptive value of circadian clocks: an experimental assessment in cyanobacteria. *Curr Biol*. 2004; 14:1481–1486. [PubMed: 15324665]
4. Drummond DA, Wilke CO. Mistranslation-induced protein misfolding as a dominant constraint on coding-sequence evolution. *Cell*. 2008; 134:341–352. [PubMed: 18662548]
5. Bulmer M. The selection-mutation-drift theory of synonymous codon usage. *Genetics*. 1991; 129:897–907. [PubMed: 1752426]
6. Plotkin JB, Kudla G. Synonymous but not the same: the causes and consequences of codon bias. *Nat Rev Genet*. 2011; 12:32–42. [PubMed: 21102527]
7. Shah P, Gilchrist MA. Explaining complex codon usage patterns with selection for translational efficiency, mutation bias, and genetic drift. *Proc Natl Acad Sci U S A*. 2011; 108:10231–10236. [PubMed: 21646514]
8. Eyre-Walker A, Bulmer M. Reduced synonymous substitution rate at the start of enterobacterial genes. *Nucl Acids Res*. 1993; 21:4599–4603. [PubMed: 8233796]
9. Akashi H. Synonymous codon usage in *Drosophila melanogaster*: natural selection and translational accuracy. *Genetics*. 1994; 136:927–935. [PubMed: 8005445]
10. Shah P, Gilchrist MA. Effect of correlated tRNA abundances on translation errors and evolution of codon usage bias. *PLoS Genet*. 2010; 6:e1001128. [PubMed: 20862306]
11. Zhou T, Weems M, Wilke CO. Translationally optimal codons associate with structurally sensitive sites in proteins. *Mol Biol Evol*. 2009; 26:1571–1580. [PubMed: 19349643]
12. Ikemura T. Correlation between the abundance of *Escherichia coli* transfer RNAs and the occurrence of the respective codons in its protein genes: a proposal for a synonymous codon choice that is optimal for the *E. coli* translational system. *J Mol Biol*. 1981; 151:389–409. [PubMed: 6175758]
13. Sharp PM, Li WH. The codon Adaptation Index - a measure of directional synonymous codon usage bias, and its potential applications. *Nucl Acids Res*. 1987; 15:1281–1295. [PubMed: 3547335]
14. Lynn DJ, Singer GA, Hickey DA. Synonymous codon usage is subject to selection in thermophilic bacteria. *Nucl Acids Res*. 2002; 30:4272–4277. [PubMed: 12364606]
15. Paul S, Bag SK, Das S, Harvill ET, Dutta C. Molecular signature of hypersaline adaptation: insights from genome and proteome composition of halophilic prokaryotes. *Genome Biol*. 2008; 9:R70.10.1186/gb-2008-9-4-r70 [PubMed: 18397532]
16. Ouyang Y, Andersson CR, Kondo T, Golden SS, Johnson CH. Resonating circadian clocks enhance fitness in cyanobacteria. *Proc Natl Acad Sci U S A*. 1998; 95:8660–8664. [PubMed: 9671734]
17. Liu Y, et al. Circadian orchestration of gene expression in cyanobacteria. *Genes Dev*. 1995; 9:1469–1478. [PubMed: 7601351]
18. Ito H, et al. Cyanobacterial daily life with Kai-based circadian and diurnal genome-wide transcriptional control in *Synechococcus elongatus*. *Proc Natl Acad Sci U S A*. 2009; 106:14168–14173. [PubMed: 19666549]

19. Vijayan V, Zuzow R, O'Shea EK. Oscillations in supercoiling drive circadian gene expression in cyanobacteria. *Proc Natl Acad Sci U S A*. 2009; 106:22564–22568. [PubMed: 20018699]
20. Vijayan V, Jain IH, O'Shea EK. A high resolution map of a cyanobacterial transcriptome. *Genome Biol*. 2011; 12:R47.10.1186/gb-2011-12-5-r47 [PubMed: 21612627]
21. Woelfle MA, Xu Y, Qin X, Johnson CH. Circadian rhythms of superhelical status of DNA in cyanobacteria. *Proc Natl Acad Sci U S A*. 2007; 104:18819–18824. [PubMed: 18000054]
22. Kudla G, Murray AW, Tollervey D, Plotkin JB. Coding-sequence determinants of gene expression in *Escherichia coli*. *Science*. 2009; 324:255–258. [PubMed: 19359587]
23. Tuller T, Waldman YY, Kupiec M, Ruppin E. Translation efficiency is determined by both codon bias and folding energy. *Proc Natl Acad Sci U S A*. 2010; 107:3645–3650. [PubMed: 20133581]
24. Gu W, Zhou T, Wilke CO. A universal trend of reduced mRNA stability near translation-initiation site in prokaryotes and eukaryotes. *PLoS Comp Biol*. 2010; 6(2):e1000664.
25. Pittendrigh CS. On Temperature Independence in the Clock System Controlling Emergence Time. *Drosophila Proc Natl Acad Sci U S A*. 1954; 40:1018–1029. [PubMed: 16589583]
26. Kondo T, et al. Circadian rhythms in prokaryotes: luciferase as a reporter of circadian gene expression in cyanobacteria. *Proc Natl Acad Sci U S A*. 1993; 90:5672–5676. [PubMed: 8516317]
27. Xu Y, Mori T, Johnson CH. Cyanobacterial circadian clockwork: roles of KaiA, KaiB and the kaiBC promoter in regulating KaiC. *EMBO J*. 2003; 22:2117–2126. [PubMed: 12727878]
28. Nakajima M, Ito H, Kondo T. *In vitro* regulation of circadian phosphorylation rhythm of cyanobacterial clock protein KaiC by KaiA and KaiB. *FEBS Lett*. 2010; 584:898–902. [PubMed: 20079736]
29. Konigsberg W, Godson GN. Evidence for use of rare codons in the *dnaG* gene and other regulatory genes of *Escherichia coli*. *Proc Natl Acad Sci U S A*. 1983; 80:687–691. [PubMed: 6338495]
30. Liu Y, Garceau NY, Loros JJ, Dunlap JC. Thermally regulated translational control of FRQ mediates aspects of temperature responses in the *Neurospora* circadian clock. *Cell*. 1997; 89:477–486. [PubMed: 9150147]
31. Sharp PM, Li WH. An evolutionary perspective on synonymous codon usage in unicellular organisms. *J Mol Evol*. 1986; 24:28–38. [PubMed: 3104616]
32. Schuster P, Fontana W, Stadler PF, Hofacker IL. From sequences to shapes and back: a case study in RNA secondary structures. *Proc Bio Sci*. 1994; 255:279–284. [PubMed: 7517565]
33. Bustos SA, Golden SS. Expression of the *psbDII* gene in *Synechococcus* sp strain PCC 7942 requires sequences downstream of the transcription start site. *J bacteriol*. 1991; 173:7525–7533. [PubMed: 1938947]
34. Xu Y, Mori T, Johnson CH. Circadian clock-protein expression in cyanobacteria: rhythms and phase setting. *EMBO J*. 2000; 19:3349–3357. [PubMed: 10880447]
35. Xu Y, et al. Intramolecular regulation of phosphorylation status of the circadian clock protein KaiC. *PLoS ONE*. 2009; 4:e7509.10.1371/journal.pone.0007509 [PubMed: 19946629]
36. Izumo M, Johnson CH, Yamazaki S. Circadian gene expression in mammalian fibroblasts revealed by real-time luminescence reporting: temperature compensation and damping. *Proc Natl Acad Sci U S A*. 2003; 100:16089–16094. [PubMed: 14657355]

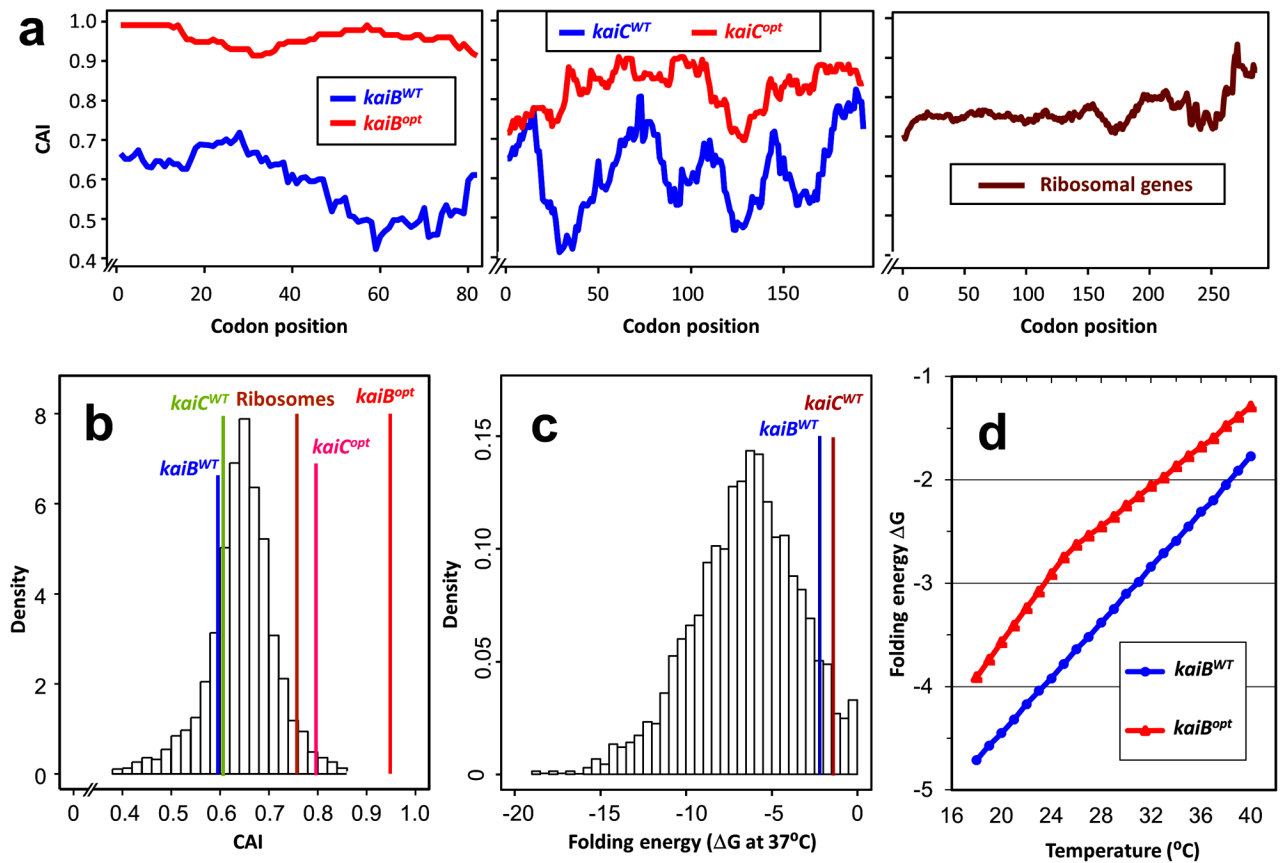


**Figure 1. Non-optimal codon usage of cyanobacterial clock genes**

**a**, Codon adaptation index (CAI) values along the entire length of different genes at a sliding window of 20 codons. Left panel: *kaiB<sup>WT</sup>* vs. *kaiB<sup>opt</sup>*; Middle panel: *kaiC* domain of *kaiC<sup>WT</sup>* vs. *kaiC<sup>opt</sup>*; Right panel: average of all ribosomal protein genes. **b**, Comparison of CAI values of the *kaiB<sup>WT</sup>*, *kaiB<sup>opt</sup>*, *kaiC<sup>WT</sup>*, *kaiC<sup>opt</sup>*, and ribosomal genes in the CAI histogram distribution of the genome. **c**, Calculated 5' folding energy of the mRNA for all genes in the *S. elongatus* genome. **d**, Comparison of calculated minimum free energy of folding ( $\Delta G$ ) over a range of temperatures between *kaiB<sup>WT</sup>* and *kaiB<sup>opt</sup>*.

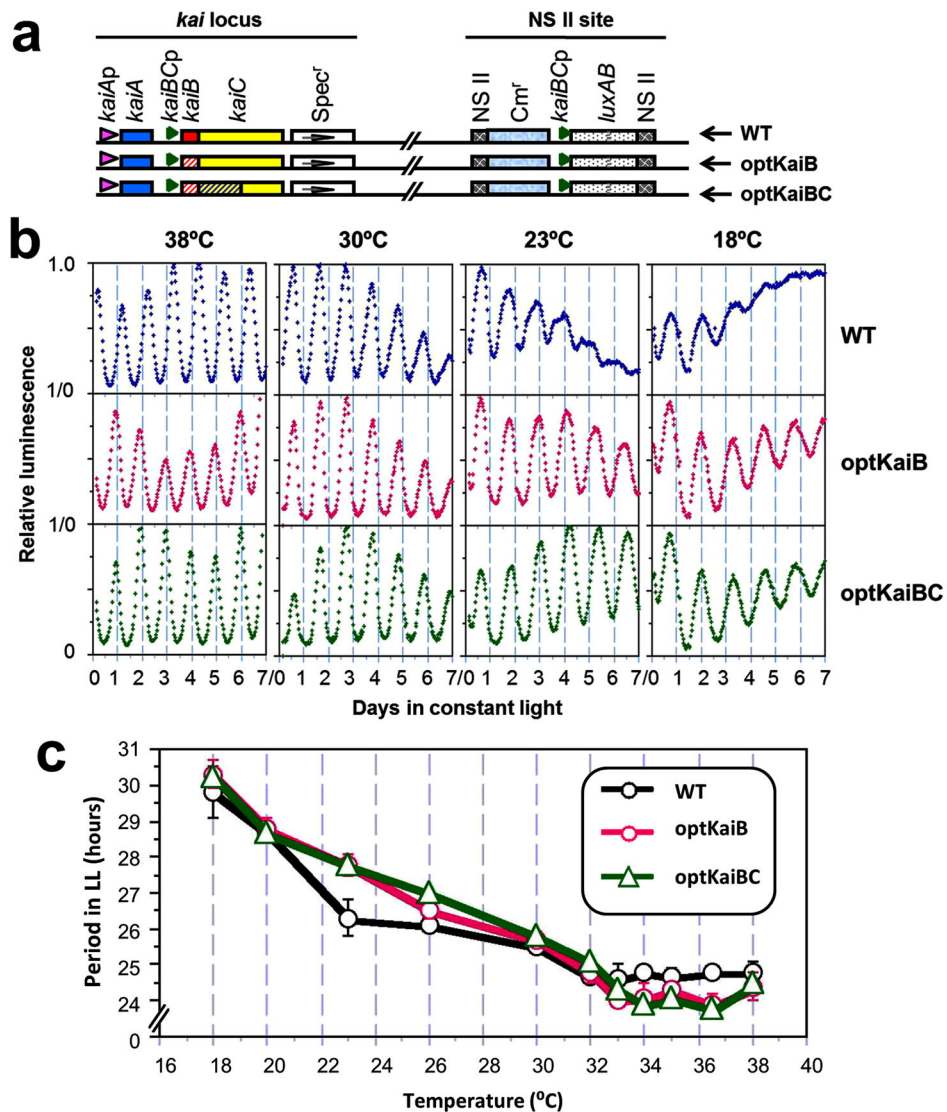


**Figure 2. Conditional circadian phenotypes of the *kai*-optimized strains**  
**a**, Diagrams of genes in the wild-type *kaiABC* (WT), *kaiB*-optimized (optKaiB), and *kaiBC*-optimized (optKaiBC) strains (see Methods for a detailed description). **b**, Luminescence rhythms of wild-type and *kai*-optimized strains in constant light at the indicated temperatures. *In vivo* luminescence rhythms were monitored from a group of 12 colonies for each strain, and a representative example is shown for each group. **c**, Free-running periods of luminescence rhythms in LL from different strains over a temperature range of 18°C to 38°C (Periods are plotted as mean ± SEM).

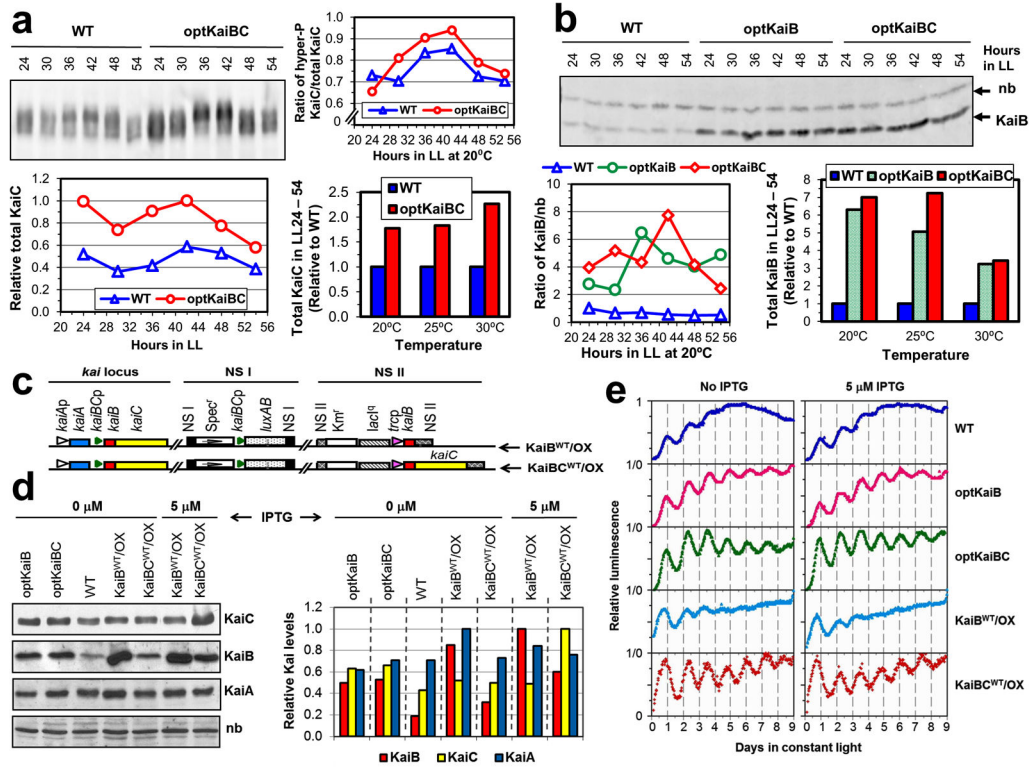


**Figure 3. Kai protein expression and circadian regulation of cells expressing wild-type versus optimized versions of *kaiBC***

**a**, KaiC immunoblots in WT and optKaiBC strains in LL at 20°C. Densitometry of the time course blots reveal the KaiC phosphorylation profiles (right panel), KaiC abundance patterns (lower left panel, relative to the maximum density band = optKaiBC at LL42), and total KaiC abundance at three temperatures (20°C, 25°C, and 30°C; lower right panel & Supplementary Fig. S1) in the optKaiBC strain from LL24 to LL54 h relative to that of WT.

**b**, KaiB immunoblots in WT, optKaiB, and optKaiBC strains in LL at 20°C. A nonspecific band (nb) was used as an internal reference for KaiB density. Densitometry of the time course blots revealed relative KaiB abundance (as the ratio of KaiB density to that of the nonspecific band, lower left panel) and total KaiB abundance at three temperatures (20°C, 25°C, and 30°C; lower right panel & Supplementary Fig. S2) in the optKaiB and optKaiBC strains from LL24 to LL54 h relative to that of WT.

**c**, Diagrams of the *kaiB<sup>WT</sup>*- or *kaiBC<sup>WT</sup>*-coexpressing strains. **d**, Elevation of KaiB and/or KaiC levels in *kaiB<sup>WT</sup>*- or *kaiBC<sup>WT</sup>*-coexpressing strains (*KaiB<sup>WT</sup>/OX* and *KaiBC<sup>WT</sup>/OX*) at LL12 with or without a low concentration (5 μM) of IPTG. The left panel shows immunoblot assays for KaiB, KaiC, and KaiA, and equal loading was confirmed by the density of the nonspecific band (nb). The right panel depicts the densitometry of the relative KaiA, KaiB, and KaiC protein abundances. **e**, Phenocopying of the cool-temperature rhythmicity of the *kaiB*- or *kaiBC*-optimized strains in the wild-type strain by increased expression of *kaiB<sup>WT</sup>* and *kaiC<sup>WT</sup>* genes. Luminescence was recorded in LL at 18°C from cultures of wild-type (WT), codon-optimized (optKaiB and optKaiBC), and *kai*-coexpressing (*KaiB<sup>WT</sup>/OX* and *KaiBC<sup>WT</sup>/OX*) strains in the presence or absence of IPTG (5 μM). Representative traces are shown for each case.

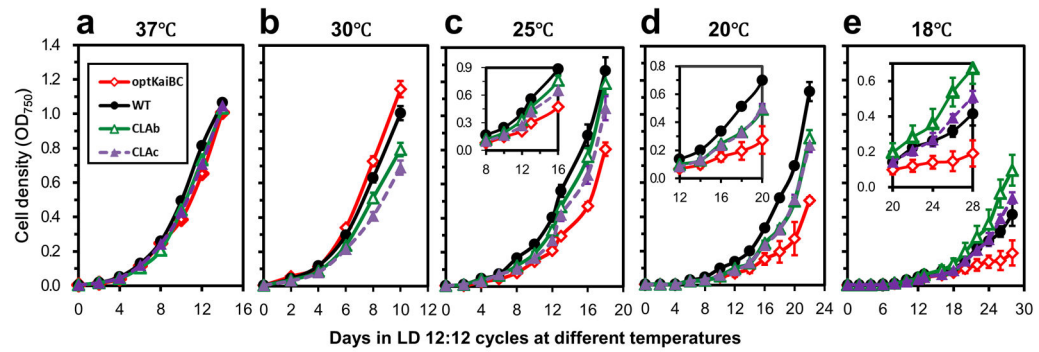


**Figure 4. Optimizing the *kaiBC* sequence causes slower growth rate at cool temperatures**  
 WT, optKaiBC, CLAb (arhythmic) and CLAc (damped oscillation) strains were grown in LD 12:12 cycles at (a) 37°C, (b) 30°C, (c) 25°C, (d) 20°C, or (e) 18°C with constant air bubbling and shaking. Cell densities were monitored by measuring OD<sub>750</sub> every two days. Data are averages  $\pm$  SEM from 2 to 6 independent experiments for each strain and condition. For a better comparison at 18°C, 20°C, and 25°C, the insets are a magnified portion for the specified times. (For doubling time calculations, see Table S7 and Supplementary Figure S5.)